Journal of Materials Science and Chemical Engineering, 2024, 12, 55-70
https://www.scirp.org/journal/msce
ISSN Online: 2327-6053
ISSN Print: 2327-6045

Fundamental Study on Alkali-Activated Slag System with Sodium Carbonate or Calcium Hydroxide

Seunghyun Na[1*], Wenyan Zhang[2], Yuichi Ichikawa[1], Masaya Komatsu[1], Aoi Takemura[1,3]

[1]Department of Architecture, Nishinippon Institute of Technology, Fukuoka, Japan
[2]School of Materials Science and Engineering, Henan Polytechnic University, Jiaozuo, China
[3]Fukuya Corporation, Fukuoka, Japan
Email: *nash@nishitech.ac.jp

How to cite this paper: Na, S., Zhang, W., Ichikawa, Y., Komatsu, M. and Takemura, A. (2024) Fundamental Study on Alkali-Activated Slag System with Sodium Carbonate or Calcium Hydroxide. *Journal of Materials Science and Chemical Engineering*, **12**, 55-70.
https://doi.org/10.4236/msce.2024.126005

Received: April 30, 2024
Accepted: June 24, 2024
Published: June 27, 2024

Abstract

Cement as a building material, has high fluidity, compressive strength, and durability, but carbon dioxide emissions during cement production are a major problem. As one of the countermeasures, alkali-activated cement using blast furnace slag powder with alkaline stimulants is considered to be a very promising solution for reducing carbon dioxide emissions, but there is a lack of information about the fundamental properties of alkali-activated materials. This study presents an experimental investigation of the fundamental properties of an alkali-activated slag system with sodium carbonate (NC) and calcium hydroxide (CH). The effects of calcium sulfo-aluminate (CSA) and shrinkage reducing agent (SRA) on the properties of blast furnace slag (BFS) based alkali-activated mixture were also investigated. In the experiments, fundamental characteristics including compressive strength, drying shrinkage, and water penetration tests of mortar were evaluated. Porosity, pH, and ignition loss were measured to verify the effectiveness of the materials. The experimental investigation revealed that the compressive strength was increased with the increasing replacement rates of NC in the BFS mortar, and in the case of water to BFS ratio of 0.45 with sodium carbonation addition contents 10 wt.%, the compressive strength for 28 days of curing reaches more than 50 MPa. Low water to BFS ratio and higher addition ratio of NC had a positive effect on the compressive strength development of mortar. Incorporating NC into BFS would affect the decrease in porosity and increase in ignition loss, leading to higher compressive strength. There was a negligible change to the compressive strength, porosity, pH, and ignition loss of BFS samples made with CH, thus, the addition rates of CH to BFS have no or little significant effect on the fundamental properties of alkali-activated cement.

From the results of drying shrinkage and water penetration tests, the addition of NC and CH only to BFS exhibited poor drying shrinkage and water penetration characteristics. However, these problems may be overcome due to the use of CSA or SRA in the alkali-activated system made with NC or CH.

Keywords

Alkali-Activated Cement, Compressive Strength, Drying Shrinkage, Water Penetration Characteristic

1. Introduction

Concrete used in the construction and civil engineering fields has many advantages to high flowability, high compressive strength, chemical resistance, water-tightness, and so on [1] [2]. Nevertheless, cement as an adhesive among concrete materials has the problem of emitting carbon dioxide during manufacturing.

Therefore, measures to utilize various industrial by-products are being actively researched to reduce cement contents. In general, industrial by-products such as BFS, fly ash, and metakaolin are used as building and civil engineering materials. When these materials are partially replaced with cement, carbon dioxide emissions can be reduced [3] [4] [5].

Recently, to further reduce carbon dioxide emissions, research on alkaline activated cement based on BFS made with NC, sodium hydroxide, and CH instead of cement has been performed specifically and implemented. The potential to apply the construction material as low-carbon society from BFS has attracted the attention of many researchers [6]-[21].

According to previous researchers, Omatsu *et al.* (2021) used inorganic salts based on sodium and calcium compounds such as $Na_2S_2O_3$, Na_2SO_4, $NaNO_3$, CaSO4, $Ca(NO_2)_2$, and $Ca(NO_3)_2$ as hardening accelerators, they have investigated the effects on the reaction and elucidation of the reaction mechanism and reported that the addition of inorganic salts increases the reaction rate of BFS powder and improves strength development [17]. Katoda *et al.* (2013) studied the hydration mechanism and hardening properties of BFS or fly ash with NC and reported that the use of the BFS-based with Na_2CO_3 aqueous solution was found to be demoldable strength [18]. More recently, Atarashi *et al.* (2022) studied the effect of the hydration mechanism of CH, sodium carbonation, and BFS. They have reported that the combination of CH and sodium carbonation significantly promotes the hydration of BFS, resulting in compressive strength development in the early period. In addition to that, it was also shown, using X-ray diffraction analysis, 8 wt.% NC only in BFS, $CaCO_3$ (calcite), $Na_2Ca(CO_3)_2 \cdot 5H_2O$(gaylussite), and C-S-H are produced up to 24 hours, and calcite and C-S-H are produced at 72 hours. Meanwhile, when CH, and NC were used in the BFS paste, the hydration products including calcite, C-S-H, and

AFm(CO_3) mono-carbonate were formed [19]. From the previous studies above, it has been shown that by using inorganic salts such as NC and CH in BFS, these materials were attributed to the hydration reaction of BFS, which is accelerated, resulting in the increase of compressive strength in the paste. The effect of two types of materials on the BFS hydration mechanism was also investigated.

Although all researchers can help and contribute to the hardening mechanism of alkali-activated cement using BFS with activators, there is little information in the literature on the fundamental properties concerning dimensional stability due to drying shrinkage and water penetration, which are closely related to long-term durability including reinforcement corrosion and scaling of the concrete structures, which is very important for expanding the long-term use of alkali-activated cement.

The objective of this study was to investigate the effect of NC and CH on the fundamental characteristics of BFS made with alkali excitation materials, including compressive strength, drying shrinkage, and water penetration. The effects of expansion materials and shrinkage-reducing agents as drying shrinkage compensation materials on the basic properties were also examined. Additionally, the effects of porosity, hydration products, and pH due to differences in material design were also examined.

2. Materials and Methods

2.1. Materials

In this study, the density of fine slag powder is 2.91 g/cm^3, the specific surface area is 4310 cm^2/g, and the content of SO_3 is 0.01%. As an alkaline activator, CH (pure more than 95.0%) or NC (pure more than 95.0%) was purchased from Hayashi Pure Chemical Ind. Ltd.; as drying shrinkage compensation materials, CSA (CSA#20, Denka CSA) and SRA (Master Life R SRA 900, Pozzolith Solutions Ltd.) were used. To compare the basic properties, two types of normal cement including ordinary Portland cement (N) and BFS cement (BB) were purchased and used in the experiment.

2.2. Mixture Proportion

Tables 1-2 show mixture proportion of mortar and paste. The ratio of water to W/BFS was 0.45 and 0.55, and CH or NC 5 or 10 wt.% was mixed with W/BFS. Two types of materials to reduce the drying shrinkage of mortar were used, 5% of CSA as expansion material was added to the BFS, and 2% of SRA was diluted in water. When manufacturing mortar, silica sand was used, and the cement-sand ratio was set to 1.5.

Table 1. Mixture proportion of mortar for the evaluating fundamental properties.

No.	Symbol	W/BFS	BFS	NC	CH	CSA	SRA
1	W45-NC5	0.45	100	5			
2	W55-NC5	0.55	100	5			

Continued

3	W45-NC10	0.45	100	10			
4	W55-NC10	0.55	100	10			
5	W45-CH5	0.45	100		5		
6	W55-CH5	0.55	100		5		
7	W45-CH10	0.45	100		10		
8	W55-CH10	0.55	100		10		
9	NC5-C0S2	0.45	100	5		5	
10	NC5-C5S0	0.45	100	5			2
11	NC5-C5S2	0.45	100	5		5	2
12	CH5-C5S2	0.45	100	5		5	2
13	N	0.45					
14	BB	0.45					

Table 2. Mixture proportion of paste for the measuring porosity, ignition loss and pH.

No.	Sym.	W/BFS	BFS	NC	CH	CSA	SRA
1	NC5	0.45	100	5			
2	NC10	0.45	100	10			
3	CH5	0.45	100		5		
4	CH10	0.45	100		10		
5	CH5-C5	0.45	100		5	5	
6	CH5-S2	0.45	100		5		2
7	N	0.45					
8	BB	0.45					

2.3. Test Methods

2.3.1. Compressive Strength

Compressive strength tests were conducted to evaluate the effect of adding each material on the compressive strength. The materials were twice mixed for 2 minutes and then cast in a prism mold with dimensions of 40 × 40 × 160 mm. After casting, the mortar samples were sealed using a lap on the top and placed at 20˚C in the experimental room for 3 days. After 3 days, the samples were de-molded and then moved into water until the planned ages at 20˚C. The compressive strength was tested according to JIS A 1108.

2.3.2. Drying Shrinkage

After casting, the mortar samples were placed in water at 20˚C until 7 days, and then mortar samples were moved to the curing room at conditions of 20 ± 2˚C and 50 ± 5%. The drying shrinkage test was performed by JIS A 1129. The initial length (L0) and initial mass (m0) were measured and set as the zero point for drying shrinkage. Length (Lt) and mass(mt) measurements were performed. Length measurements were conducted using a micrometer (1/1000 mm). The drying shrinkage rate was calculated by using the formula: (L0-Lt)/L0.

2.3.3. Water Penetration Depth

The water penetration depth was measured by JSCE-G 582-2018. The materials were cast in cylinder mold with dimensions of 50 × 100 mm and then sealed using a plastic vinyl bag. The mold was placed in a container at a condition of 20˚C. After 28 days, the samples were dried at 40˚C until 56 days. The weight loss of each mortar sample was measured before and after high temperature. After drying, all mortar samples were placed in the experimental room for 6 hours. After taping the sides of the test samples, they were immersed in water for part of 10 mm from the bottom surface. The sample was also immersed in water for 2 days and split using the universal testing machine. Then, the water penetration depth of the mortar test was measured using a simple water spray. Additionally, the weight of the mortar sample before and after water immersion was measured to compare the results of water penetration depth.

2.3.4. pH Value

Here, paste samples were prepared. Each material was mixed for about 5 minutes using a hand mixer and then placed into a silicone mold with a dimension of 75 × 75 × 5 mm. Afterward, they were de-molded after 3 days and stored in a container at 20˚C in water. At 7, 21, and 28 days of age, the samples were moved to an oven at 40˚C and dried for 1 day. Then, the paste was pulverized to less than 150 micrometers. The liquid-to-solid ratio was 5, and after mixing for about 2 minutes by hand, the pH value was measured using a pH meter (DKK-TOA CO., HM-30P) after 60 minutes.

2.3.5. Porosity

To assess the change in the porosity of the paste due to the addition of each material, Archimedes' porosity was measured. After manufacturing the paste in the same manner as the pH test, they were placed in water at 20˚C. Then, before testing, the hydration of the paste was stopped using ethanol. Afterward, it was dried at 40˚C for 1 day to dry the ethanol. Then, using a vacuum pump, the paste was immersed in water for 1 day to measure the weight of underwater and surface dry. Then, the paste samples were stored at 40°C for 1 day and their dry weight was measured.

2.3.6. Ignition Loss

An ignition loss was measured to evaluate the change of hydration reaction with curing age and different mixtures. The method of the paste system was the same as that of the pH test, the hydration of the paste was stopped using ethanol, and paste samples were dried at 40˚C for 1 day. Then, the paste was pulverized to less than 150 micrometers, and 1 to 2 grams of paste was placed in the furnace for 30 mins. The temperature ranged between 40˚C to 300˚C and the ignition loss was calculated using the formula: $(m_{40} - m_{300})/m_{40} \times 100$.

3. Results

3.1. Compressive Strength

Figure 1 shows the results of the compressive strength for the alkali activated blended mortar samples with different alkali materials of NC or CH ratios 5 and 10 wt.%, and water to BFS ratio was also evaluated. It was found from the Figure 1(a) that in case of high NC contents and low water to BFS ratio, the compressive strength increases with increasing the curing age and NC contents, indicating that the incorporation of NC and low water to BFS ratio in the mortar sample has a positive effect on the increasing compressive strength characteristics. It is because that NC could promote and accelerate the hydration of BFS and consequently increase the compressive strength. This will be further discussed in the discussion part.

However, it can be seen from Figure 1(b) that, in the case of different CH contents and water to BFS ratio, the compressive strength has the same tendency despite the CH contents or water contents were different, which implies that these parameters would not affect the compressive strength in the mortar.

Figure 1(c) and (b) present the compressive strength of mortar with CSA or SRA at the same NC contents of 5 wt.%. In the case of CSA of 5 wt.% (C5), it was found that the compressive strength at 7 days of age was low, but no significant difference could be confirmed at 28 days of age, which is considered that hydration of NC and BFS would be delayed by addition to the CSA at the early age.

As can be seen form Figure 1(b), it is found that there is no significant difference among different contents of SRA. This indicates that the SRA contents probably have a negligible effect on the compressive strength of NC mortar.

Figure 1(e) shows the effects of CSA and SRA on the compressive strength of mortar containing alkaline stimulants. As can be seen from the figure, in the case of the NC5-C5S2 mortar sample, it was confirmed that the compressive strength decreased slightly at 7 and 28 days compared to the NC5 sample without CSA and SRA. As mentioned above, the decrease of compressive strength in NC5-C5-S2 was not evident in this study. This behavior should be existed and needed for further investigation.

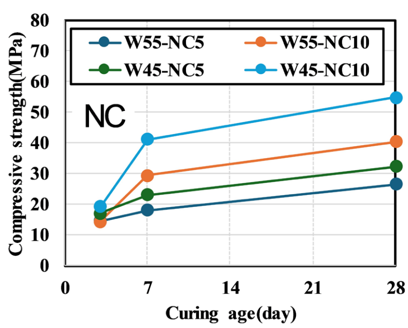

(a) NC

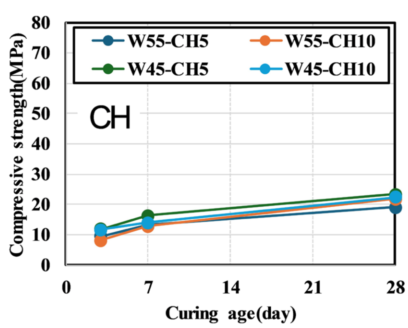

(b) CH

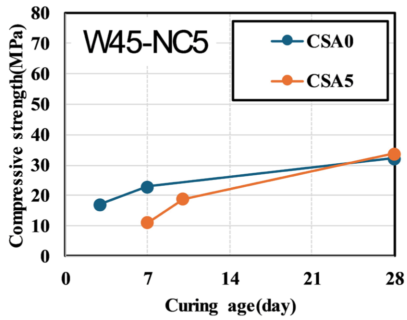

(c) CSA

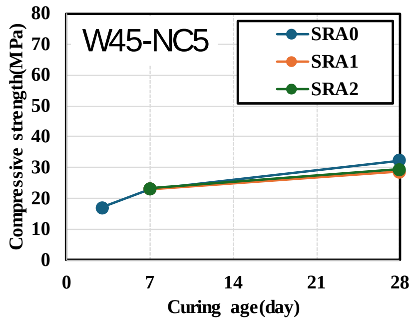

(d) SRA

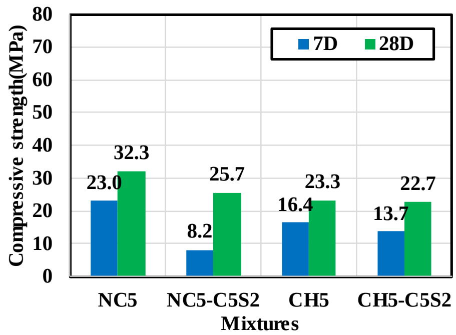

(e) Effect of CSA and SRA

Figure 1. Compressive strength of mortar.

3.2. Drying Shrinkage and Weight Loss

Figures 2-4 show the results of the drying shrinkage for the alkali-activated blended mortar when the ratio of alkali materials (NC, CH) is 5 wt.% with 0.45 of W/BFS. In addition, the effect of CSA and SRA on the NC or CH system was also investigated. All mortar samples were exposed to 20˚C at 60% RH. It was confirmed that the drying shrinkage of the mortar samples was decreased with the extension of the drying age. At the drying age of 84 days, the shrinkage amount was −3287 and −3778 for the CH5 and NC5 mortar samples, but the weight loss for each sample was similar. It is confirmed from the drying shrinkage test result that the addition of NC was more likely to cause drying shrinkage compared to the addition of CH.

Figure 3 shows the drying shrinkage test results of 5% NC mortar containing CSA and SRA. At 84 days of age, when 5% CSA was added to NC, the drying shrinkage was −3430 and −2325 × 10^{-6} for the samples of NC5-C5S0 and NC5-C0S2. A slight reduction is observed in NC5-C5S0 in comparison to NC5-C0S0. Additionally, with the addition of CSA and SRA, the drying shrinkage of C5S2 was 2092 × 10^{-6}. This indicates that the combination of CSA and SRA had a positive effect on dimensional stability.

As can be seen in Figure 4, in the case of mortar containing CH, similar results to that in Figure 3 were observed. It was found that the drying shrinkage was −1041 × 10^{-6} and a significant reduction of drying shrinkage was observed for CH5-C5S2. This trend corresponds to the results of the weight loss of the

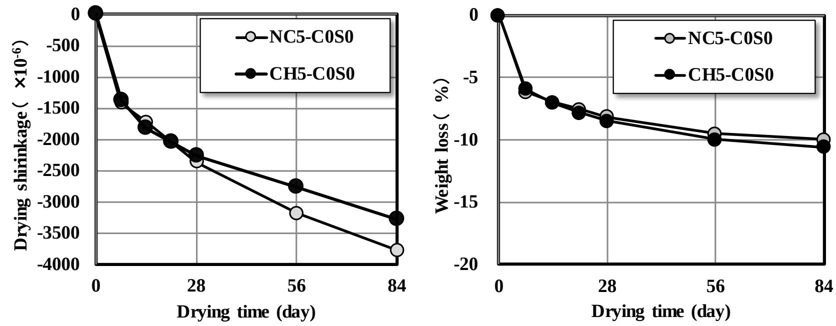

(a) Drying shrinkage (b) Weight loss

Figure 2. Drying shrinkage of NC and CH.

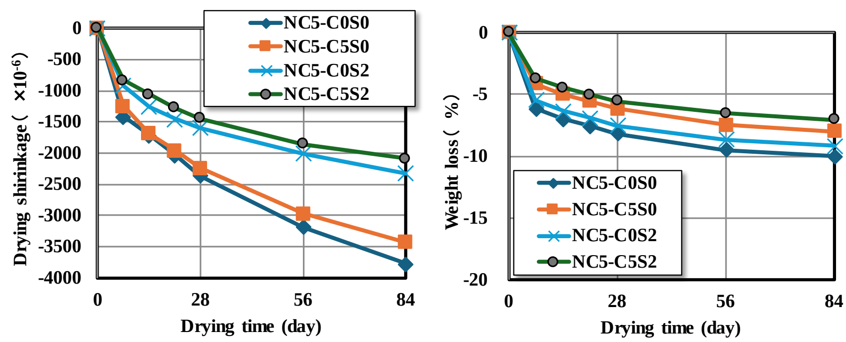

(a) Drying shrinkage (b) Weight loss

Figure 3. Drying shrinkage of NC with CSA and SRA.

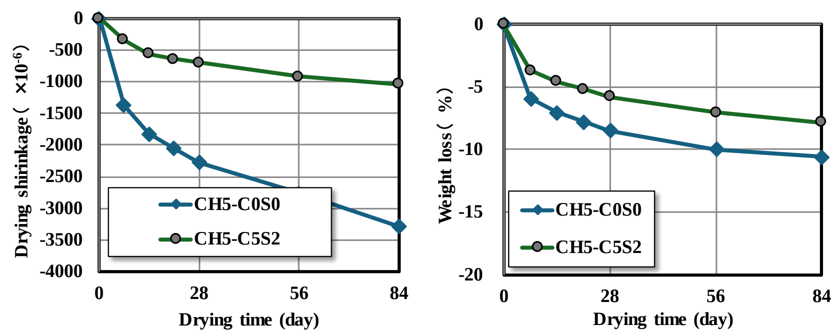

(a) Drying shrinkage (b) Weight loss

Figure 4. Drying shrinkage of CH with CSA and SRA.

mortar during the drying period. From the results above, it is concluded that the addition of NC or CH only to BFS may be susceptible to drying shrinkage and can cause poor resistance to drying. However, this can be compensated effectively and improved by using the combination of CSA and SRA in the mortar samples.

3.3. Water Penetration Characteristics

3.3.1. Water Content Change before Test

To evaluate the moisture penetration characteristics of alkaline-activated cement, the test specimen was de-molded after sealing and curing for 28 days. Afterward, the mortar sample was dried at 40˚C for 28 days. In addition, the weight change of the test specimen during this drying process was measured. Figure 5 presents the weight change result of all mortar samples before and after drying at 40˚C. As can be seen in Figure 5, the weight of the mortar was changed from −4.5 to −10.0% after drying. In the case of NC5 or CH5 mortar samples containing NC and CH alone, the moisture evaporation contents were found to be −9.5% or −8.7%, which was lower than that of N and BB.

In comparison to NC5 and CH5 mortar samples, it was found that the water evaporation amount was −5.1% and −4.5% for NC5-C5S2 and CH5-C5S2, respectively. The water evaporation content of those mixtures was lower than that of other mortar samples. This implies that CSA and SRA can contribute to the decreasing water evaporation content.

3.3.2. Water Penetration Depth

Figures 6-7 show the results of the water penetration depth for the alkali-activated blended mortar with different mixtures. As can be seen in Figure 6, in the case of normal cement of N and BB, it was confirmed that the water penetration depth was 44.6 and 17.5 mm, implying that the water penetration depth of BB cement is relatively low. This is due to the densification of the microstructure of BB cement.

For the alkali-activated mortar samples, the water penetration depth of NC5 was found to be almost 100 mm. This result indicates that incorporating NC of 5 wt.% only exhibits poor water penetration resistance compared to the normal cement of N and BB.

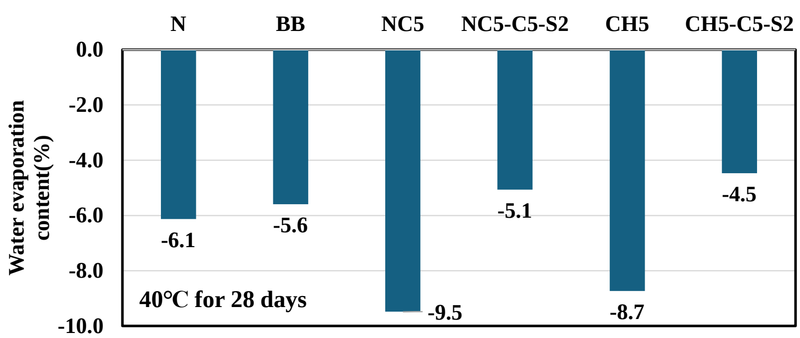

Figure 5. Water evaporation contents at 40˚C before water penetration test.

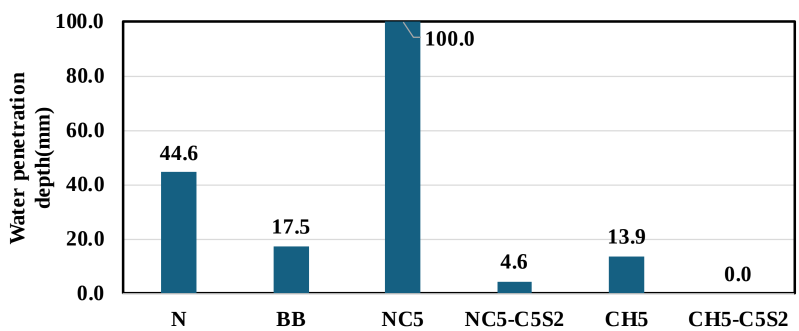

Figure 6. Water penetration depth.

Meanwhile, the water penetration depth of CH5 mortar was recorded to be 13.9 mm and is lower than that of normal cement of N and BB, which implies that a more significant decrease in water penetration depth was observed in CH5 mortar. For incorporating CSA and SRA mortar, the water penetration depth for NC5-C5S2 and CH5-C5S2 was 4.6 and 0 mm, significantly lower than that of other mortar samples, suggesting that the addition of CSA and SRA has a positive impact on the water penetration properties.

3.3.3. Water Penetration Content before and after 48 Hours

Figure 8 presents the results of the water penetration content of the mortar sample. The results showed that the weight of moisture in the samples containing NC, NC5, and NC5-C5-S2, was 11.4 and 6.8%, and the amount of moisture penetration was high compared to other samples. This indicates that water can penetrate the NC-based mortar sample.

3.4. pH Result

The PH measurement results of each paste sample are shown in Figure 9. The pH of N and BB, which are normal cement and BB cement, was measured to be 12.6 to 12.7. It was thought to be caused by the CH from the hydration product of cement and potassium oxide or sodium oxide from cement. Other samples containing NC and CH were confirmed to have pH values of 12.2 to 12.6, similar to or slightly lower than that of normal cement. The pH of NC5 with 5 wt. % NC

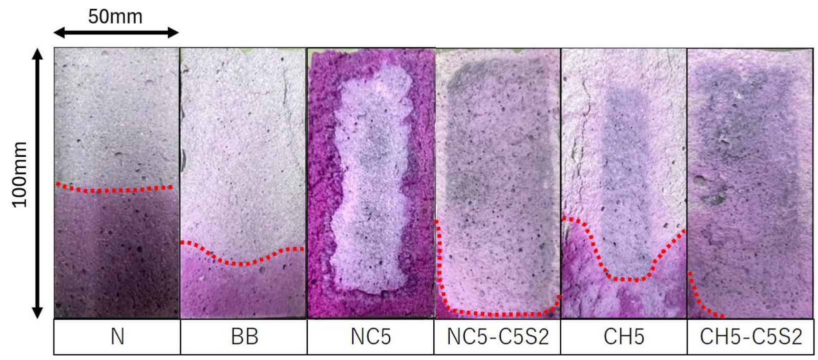

Figure 7. Mortar samples after water penetration test.

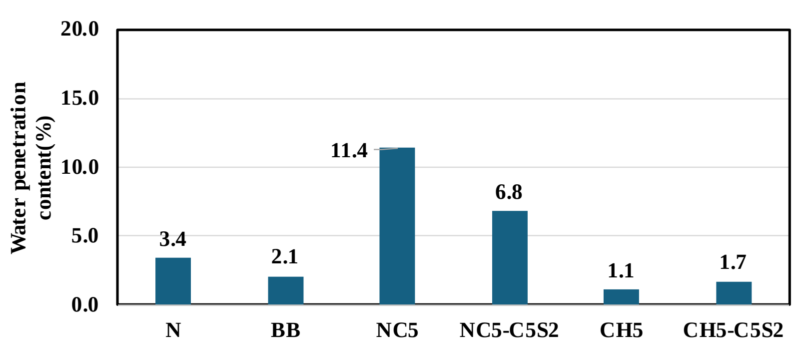

Figure 8. Water penetration contents after 48 hrs.

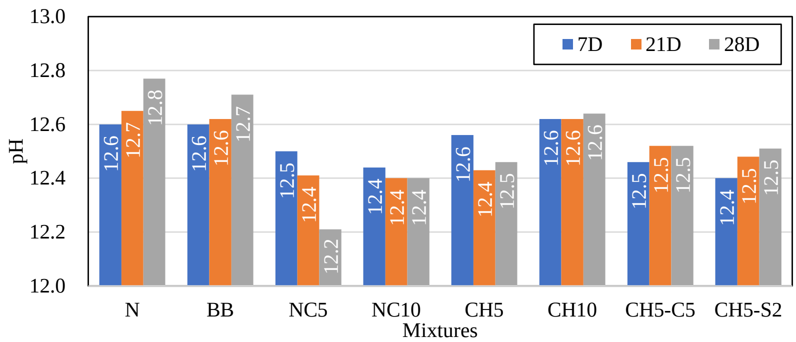

Figure 9. Change of pH for paste samples.

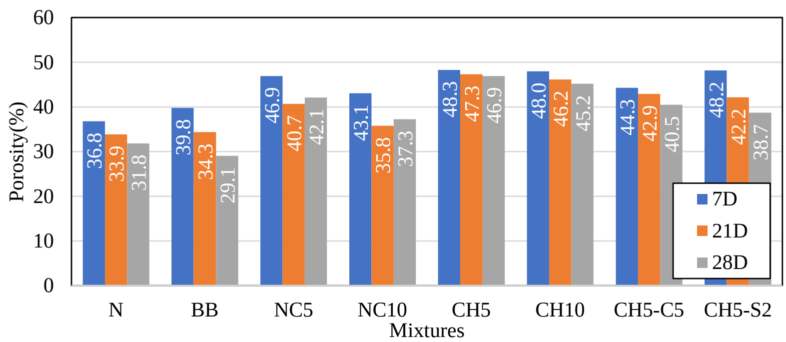

Figure 10. Change of porosity for paste samples.

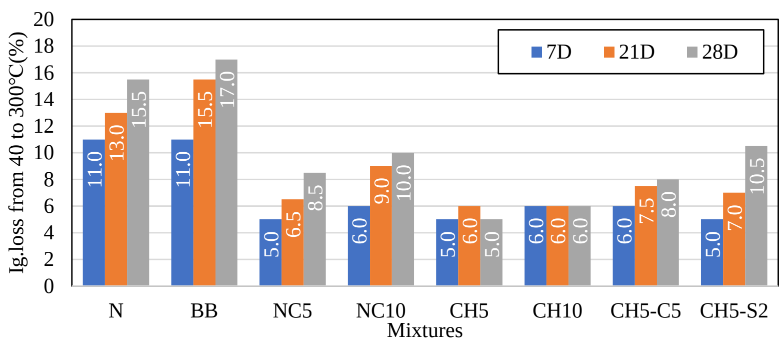

Figure 11. Change of ignition loss for paste samples.

decreased slightly with increasing age from 7 to 28 days. This may be due to the hydration reaction of BFS with NC, resulting in a decrease in the pH value of the system during hydration. In addition, in the case of CH5-C5 and CH5-C2 containing CSA and SRA, the pH is measured to be 12.4 to 12.5, indicating that the use of these materials does not affect the pH of CH-based paste.

3.5. Porosity

Figure 10 shows the results of porosity measurement using the Archimedes method. The porosity of N and BB pastes was found to decrease gradually with the increase of curing age, and the porosity of N and BB at 28 days of age was measured to be 31.8% and 29.1%, which was mainly affected by hydration reaction.

At 28 days of age, the porosity of NC5 and NC10 containing NC was 42.1% and 37.3%, and the porosity of CH5 and CH10 containing CH was 46.9% and 45.2%, respectively. With the same additional amount, the porosity of the paste containing calcium carbonate was lower than that of the sample containing CH. From the above results, it is concluded that NC is more effective in densification of pore structure compared to CH.

In addition, the porosity of the CH5-C5 or CH5-S2 sample prepared with CH with the CSA and SRA was measured to be 40.5% and 38.7%, which are lower than that of the CH5 sample, implying that CSA and SRA can contribute to the decreasing porosity.

3.6 Ignition Loss

In this paper, the effect of NC, CH, CSA, and SRA on the hydration products of BFS was investigated, and the amount of change of residual water and hydration products, such as C-S-H, Ettringite, and Mono-sulfate were evaluated. The result was obtained from an average of three paste samples.

Figure 11 shows the results of ignition loss from 40˚C to 300˚C. In the case of common cement of N and BB, the ignition loss was found to increase with the increase of curing age, which was thought to be due to the progress of cement hydration reaction. This increasing tendency for ignition loss was similar to the NC5 and NC10 paste samples. However, in CH5 and CH10 pastes containing CH, the ignition loss was measured at 5 - 6%, and ignition loss does not change with the increase of curing age, which implies that contents of CH may not affect the hydration reaction with BFS. From this result, the hydration reaction of CH with BFS may not effectively occur. In addition, at the curing age of 28 days, the ignition loss of the CH5-C5 or CH5-S2 sample was measured to be 8.0% and 10.5% higher than that of the CH5 sample, implying that CSA and SRA can contribute to the decreasing porosity.

4. Discussion

4.1. Effect of Stimulants

4.1.1. NC

From the results of the compressive strength test, as shown in **Figure 1**, it was confirmed that the compressive strength of mortar samples with low W/BFS and high NC addition content is approximately 40 MPa or more at 28 days. The increase in compressive strength is generally related to the porosity and ignition loss of the hydration product in the matrix. From the results of porosity and ignition loss given in **Figures 10-11**, it was confirmed that the mixtures made with BFS and NC had a low porosity and a high loss on ignition.

Therefore, to summarize the results obtained from this study, in the mixtures based on BFS and NC, the hydration reaction of BFS can be improved by adding NC. It is also concluded that BFS reacts with NC to form hydration products, which can fill the voids in the hydration product, resulting in increasing the compressive strength.

Meanwhile, as can be seen in **Figure 9**, the pH measurement results of the sample containing 5% NC with BFS were confirmed to have a low pH compared to BB as general cement. Miyahara *et al.* conducted a hydration reaction analysis of NC and BFS and they reported that C-S-H with a low calcium silicate ratio is generated through the hydration reaction of NC and BFS and that sodium ions as a stimulant are absorbed into C-S-H [21]. It is considered that these hydration reaction products are probably related to the pH results measured in this study.

4.1.2. CH

The compressive strength results showed that with the increase of CH content to the BFS, the compressive strength at the age of 28 days was approximately 22 to 23 MPa, as given in **Figure 1**. Further, in the porosity and ignition loss tests, there is no significant change in porosity and ignition loss, as shown in **Figures 10-11**. From the results above, this study suggests that the effect of the proportion of CH added to BFS on the compressive strength and hydration of BFS may be negligible. In addition, from the perspective of water penetration depth, as shown in **Figure 6**, the water penetration depth results show that when only NCorCH is added, the water penetration depth is higher than that of common cement such as N and BB.

Meanwhile, in the case of samples containing CH, a lower water penetration depth was confirmed than that of NC, as shown in **Figure 6**. However, as shown in **Figure 1** and **Figure 11**, the sample containing NC has higher compressive strength and slightly lower porosity in comparison to CH. This trend contrasts with the water penetration depth results. One of the reasons for this result may be that CH, which has a high specific surface area, remains in a not completely dissolved state, resulting in the change of the pore structure.

In addition, the weight evaporation contents of the hardened mortar sample containing NC before the water penetration test is slightly higher than that of CH. This suggests that the water inside the mortar sample is evaporated easily. The evaporation of water from the inside to the outside of this hardened mortar has the potential to cause significant drying shrinkage. However, in this study, the test of drying shrinkage at high temperatures for alkaline activated cement has not been performed, thus, additional research is needed on quantitative dimensional stability in high-temperature environments and water movement during moisture movement.

4.2. Effects of CSA and SRA

From the results of drying shrinkage, it could be found that when CSA was added to the BFS and NC mixture in the water curing process, the compressive strength at 7 days of age was reduced, as shown in **Figure 1**. Although the reason for this behavior is not clear in this study, it is assumed that the reaction between the NC and the BFS is slightly delayed in the presence of CSA, which should be further investigated. Furthermore, it was revealed that the dimensional stability of BFS is low when only NC or CH is added. However, this may be overcome by the use of CSA and SRA, and the combination of these materials in BFS systems with NC or CH can improve resistance to drying. Although outside the scope of this study, it is considered that this reduction in drying shrinkage is due to the formation of ettringite and the reduction of surface tension, as well as changes in pore structure [22] [23] [24].

5. Conclusions

1) The compressive strength test results confirmed that the addition of NC increased the compressive strength compared with CH. In addition, according to the test results of the porosity and ignition loss of cement paste containing NC, it is confirmed that the porosity decreased and the ignition loss tended to increase.

2) The pH test results showed that the pH value of all investigated paste was 12.4 to 12.7, except for the formulation with 5% NC added, which is approximately the same value compared to N and BB. On the other hand, when the NC content is 5%, the pH when the NC content is 5% tends to decrease with the increase of the curing age.

3) From the test results of compressive strength, porosity, and loss on ignition, it was found that the compressive strength of BFS samples added with CH did not change significantly despite the increase of the addition rate, and the porosity and the ignition loss also showed a similar tendency. Therefore, it was assumed that the addition of CH has little effect on the compressive strength of the BFS.

4) The results of the drying shrinkage test show that the dimensional stability of the mortar sample prepared by adding NC and CH to the BFS is low, but the combined use of CSA and SRA can improve its dimensional stability. These are significantly effective for the drying shrinkage of mortar.

5) Adding NC and CH to the BFS mortar sample, the water penetration depth was significantly increased. On the other hand, it was confirmed that the water penetration depth tends to become smaller when CSA and SRA are used together in the mortar.

Acknowledgements

The authors gratefully acknowledge the start-up research foundation of the Nishinippon Institute of Technology. We also would like to thank Mr. Masaki Oshima (Pozzolith Solutions Ltd.) and Mr. Yuya Hashimoto (Nippon Steel Slag Products Co. Ltd.) for supplying the materials of shrinkage reducing agent or blast furnace slag powder for this research.

Conflicts of Interest

The authors declare no conflicts of interest regarding the publication of this paper.

References

[1] Kobayash, T. and Koji, K. (2015) Latest Concrete Engineering. 6th Edition, Morikita Publishing, Tokyo.

[2] Matsumoto, S. (2019) Revised Edition Illustrated Guide Easy Building Materials. Gakugei Shuppansha, Kyoto.

[3] Sun, J., Hou, S., Guo, Y., He, W., Bao, J., Cui, Y., *et al.* (2024) Sustainable Utilization of Alkali-Activated Steel Slag Material: Effects of Silicate Modulus and GBFS on Fresh, Mechanical and Pore Structure Properties. *Developments in the Built Environment*, **18**, Article ID: 100410. https://doi.org/10.1016/j.dibe.2024.100410

[4] De Filippis, U., Prud'homme, E. and Meille, S. (2021) Sodium Hydroxide Substitution in Slag Activating Mixes: A Potential Pathway to More Sustainable Slag-Based Binders. *Construction and Building Materials*, **300**, Article ID: 124183. https://doi.org/10.1016/j.conbuildmat.2021.124183

[5] Wang, J., Lyu, X., Wang, L., Cao, X., Liu, Q. and Zang, H. (2018) Influence of the Combination of Calcium Oxide and Sodium Carbonate on the Hydration Reactivity of Alkali-Activated Slag Binders. *Journal of Cleaner Production*, **171**, 622-629. https://doi.org/10.1016/j.jclepro.2017.10.077

[6] Dai, X., Aydın, S., Yardımcı, M.Y., Lesage, K. and Schutter, G.D. (2021) Effect of $Ca(OH)_2$ Addition on the Engineering Properties of Sodium Sulfate Activated Slag. *Materials*, **14**, Article No. 4266. https://doi.org/10.3390/ma14154266

[7] Akturk, B., Kizilkanat, A.B. and Kabay, N. (2019) Effect of Calcium Hydroxide on Fresh State Behavior of Sodium Carbonate Activated Blast Furnace Slag Pastes. *Construction and Building Materials*, **212**, 388-399. https://doi.org/10.1016/j.conbuildmat.2019.03.328

[8] Adesina, A. (2020) Influence of Various Additives on the Early Age Compressive Strength of Sodium Carbonate Activated Slag Composites: An Overview. *Journal of the Mechanical Behavior of Materials*, **29**, 106-113. https://doi.org/10.1515/jmbm-2020-0011

[9] Akturk, B. and Kizilkanat, A.B. (2020) Improvement of Durability and Drying Shrinkage of Sodium Carbonate Activated Slag through the Incorporation of Calcium Hydroxide and Sodium Hydroxide. *Construction and Building Materials*, **243**, Article ID: 118260. https://doi.org/10.1016/j.conbuildmat.2020.118260

[10] Jiao, Z., Wang, Y., Zheng, W. and Huang, W. (2018) Effect of Dosage of Sodium Carbonate on the Strength and Drying Shrinkage of Sodium Hydroxide Based Alkali-Activated Slag Paste. *Construction and Building Materials*, **179**, 11-24. https://doi.org/10.1016/j.conbuildmat.2018.05.194

[11] Duan, K., Liu, Z., Li, X., Wang, D., Cao, W. and Zhao, Y. (2024) Understanding the Role of Calcium Silicate Slag in Sodium Carbonate-Activated Green Materials: Influence on Kinetics, Strength, and Efflorescence. *Journal of Cleaner Production*, **450**, Article ID: 141924. https://doi.org/10.1016/j.jclepro.2024.141924

[12] Tang, D., Yang, C., Li, X., Zhu, X., Yang, K. and Yu, L. (2021) Mitigation of Efflorescence of Alkali-Activated Slag Mortars by Incorporating Calcium Hydroxide. *Construction and Building Materials*, **298**, Article ID: 123873. https://doi.org/10.1016/j.conbuildmat.2021.123873

[13] Kim, T. (2012) The Strength Properties of Alkali-Activated Slag Mortars by Combined Caustic Alkali with Sodium Carbonate as Activator. *Journal of the Korea Concrete Institute*, **24**, 745-752. https://doi.org/10.4334/jkci.2012.24.6.745

[14] Yang, K., Cho, A. and Song, J. (2012) Effect of Water-Binder Ratio on the Mechanical Properties of Calcium Hydroxide-Based Alkali-Activated Slag Concrete. *Con-*

struction and Building Materials, **29**, 504-511. https://doi.org/10.1016/j.conbuildmat.2011.10.062

[15] Dai, X., Ren, Q., Aydin, S., Yardimci, M.Y. and De Schutter, G. (2023) Accelerating the Reaction Process of Sodium Carbonate-Activated Slag Mixtures with the Incorporation of a Small Addition of Sodium Hydroxide/Sodium Silicate. *Cement and Concrete Composites*, **141**, Article ID: 105118. https://doi.org/10.1016/j.cemconcomp.2023.105118

[16] Omatsu, H., Yamada, Y. and Kurumisawa, K. (2021) Effect of Inorganic Salts on Strength Development of Hardened Blast Furnace Slag. *Cement Science and Concrete Technology*, **74**, 44-50. https://doi.org/10.14250/cement.74.44

[17] Kadota, H., Atarashi, D., Horiguchi, K. and Sakai, E. (2013) Solidification of Na_2CO_3 Solution by Blast Furnace Slag and Fly Ash. *Cement Science and Concrete Technology*, **67**, 52-58. https://doi.org/10.14250/cement.67.52

[18] Atarashi, D., Yoshida, R., Itoh, T. and Osaki, M. (2023) Influnence of Calcium Hydroxide on the Reaction of Blast Furnace Slag Paste with Sodium Carbonate. *Cement Science and Concrete Technology*, **76**, 101-107. https://doi.org/10.14250/cement.76.101

[19] Zhang, W., Jin, Y., Na, S., Zhao, L., Su, F. and Zhu, J. (2024) Improving Mechanical Properties of Hemihydrate Phosphogypsum via Alkali-Activated Mineral Admixtures. *Journal of Cleaner Production*, **454**, Article ID: 142234. https://doi.org/10.1016/j.jclepro.2024.142234

[20] Na, S., Lee, W. and Song, M. (2021) Hardening Properties of Foamed Concrete with Circulating Fluidized Bed Boiler Ash, Blast Furnace Slag, and Desulfurization Gypsum as the Binder. *Open Journal of Civil Engineering*, **11**, 301-316.

[21] Miyahara, S., Okamoto, R., Takeda, H. and Sakai, E. (2015) C-S-H Composition of Slag Past Activated by Na_2CO_3. *Cement Science and Concrete Technology*, **69**, 69-75.

[22] Yamamoto, K., Morioka, M., Sakai, E. and Daimon, M. (2003) Expansion Mechanism of Cement Added with Expansive Additive. *Concrete Research and Technology*, **14**, 23-31. https://doi.org/10.3151/crt1990.14.3_23

[23] Narumi, R., Zhang, W., Kishimoto, Y. and Hama, Y. (2014) Investigation of Affecting Factors on Reductance of Drying Shrinkage and Degradation of Frost Resistance of Mortar with Shrinkage Reducing Agent. *Journal of Structural and Construction Engineering* (*Transactions of AIJ*), **79**, 671-680. https://doi.org/10.3130/aijs.79.671

[24] Zhang, W., Duan, X., Su, F., Zhu, J. and Hama, Y. (2024) Drying Shrinkage Inhibition Effect and Mechanism of Polyol Shrinkagex Reducing Admixture on the Metakaolin-Based Geopolymer. *Journal of Materials Research and Technology*, **28**, 2021-2032.